PCCP

Surface species formed during UV photolysis of ozone adsorbed on water ice films at 80 K. A combined RA-FTIR and DFT study

Stanislav K. Ignatov,*[ab] Petr G. Sennikov,[ac] Hans-Werner Jacobi,[a] Alexei G. Razuvaev[b] and Otto Schrems[a]

[a] *Alfred Wegener Institute for Polar and Marine Research, Bremerhaven, Germany. E-mail: oschrems@awi-bremerhaven.de; Fax: 49 471 4831 1425; Tel: 49 471 4831 1480*
[b] *University of Nizhny Novgorod, 23 Gagarin Avenue, Nizhny Novgorod 603600, Russia. E-mail: ignatov@ichem.unn.runnet.ru; Fax: 07 8312 658592; Tel: 07 8312 658035*
[c] *Institute of Chemistry of High-Pure Substances, 49 Tropinin Str., Nizhny Novgorod 603600, Russia. E-mail: sen@ihps.nnov.ru; Fax: 07 8312 668666; Tel: 07 8312 658035*

Received 23rd August 2002, Accepted 6th December 2002
First published as an Advance Article on the web 23rd December 2002

The reflection–absorption FTIR spectra of the ozone–water films deposited on a cold metallic surface at 80 K before and after irradiation at 250 and 320 nm were studied to model the ozone photolysis and superoxidant adsorption taking place on the ice particles in the Earth's atmosphere. A new sharp intense band at 2860 cm^{-1} and a low-intense band at 1450 cm^{-1} were observed after irradiation at both wavelengths together with remarkable reshaping of the ice *Ih* bands in the regions 3100–3600 cm^{-1} and 500–1000 cm^{-1}. The annealing of the reaction mixture has small effect on the intensities and positions of the new bands. The adsorption of formed species was modelled by DFT cluster calculations. The species $O(^1D)$, $O(^3P)$, $O_2(a\ ^1\Delta_g)$, $O_2(X\ ^3\Sigma_g)$, $HO^\bullet$, $HOO^\bullet$, H_2O_2 were considered as possible intermediates and products. Among them, $HO^\bullet$, H_2O_2, and $HOO^\bullet$, form hydrogen bound complexes with estimated binding energies of −17.6, −28.5, and −37.2 kJ mol^{-1}, correspondingly. The observed IR band of 2860 cm^{-1} can not be assigned to the OH vibrations of H_2O_2 shifted due to the adsorption and it is assigned to the $\nu_2+\nu_6$ combination band of H_2O_2. Apart from H_2O_2, two other species can absorb in the region 2700–2900 cm^{-1}: the adsorption complex of $HOO^\bullet$ on the ice surface and $O(^1D)$ forming the complex with the ice of oxywater structure $O\cdots OH_2$ stabilized by additional hydrogen bonds.

Introduction

The gas-phase reactions of ozone in the Earth's atmosphere and the role of these reactions in various atmospheric phenomena including ozone depletion, formation of polar stratospheric clouds and the ozone-conservation cycles were abundantly studied in the last two decades and well-documented today.[1] In contrast, the role in these processes of small atmospheric particles including the industrial aerosols, the interstellar dust and, especially, the small particles of the atmospheric ice is up to now only poorly understood. Nevertheless, these particles can have a remarkable effect on the atmospheric chemistry because reactions occurring at their surface can have quite different kinetic and thermodynamic parameters than those in the gas phase.[2] In particular, the photolytic decomposition of ozone and the subsequent reactions of formed products is an example of a process which can be dramatically influenced by the ice surface. This process is of special importance because of its effect on the atmospheric transport of superoxidants, and the superoxidant accumulation in the snow and ice cover in the polar regions and Siberia. The importance of possible stabilization of superoxidants formed in the photolysis due to the adsorption on the ice surface and the ability of the ice surface to transfer and accumulate them motivates studying the ozone photolysis on the surface of water ice. In this work, a laboratory modelling study of the UV induced ozone photodecomposition and related reactions under conditions comparable to conditions in the Earth's atmosphere was undertaken by means of IR spectroscopy and DFT calculations with emphasis on adsorption complexes of superoxidants formed in the course of photolysis.

Recently, ice surface deposition experiments were carried out including adsorption of ozone,[3–5] water,[6] carbon monoxide and methane,[7] methanol, acetone, and acetaldehyde.[8] The IR spectra of ozone in the adsorbed state were studied leading to the conclusion that the ozone molecule only interacts with the ice surface physically, resulting basically in changes in the dangling OH group frequencies.[3,4] The photolysis of ozone in the presence of water was studied under matrix isolation conditions.[9,10] It was found that the photolysis at 308 nm resulted in the formation of H_2O_2 with small amounts of $HOO^\bullet$ and $HO^\bullet$. It was shown earlier that the photolysis of solid ozone at 308 nm in excess ice also resulted in H_2O_2 formation.[11] However, the possibility of the formation of reactive superoxidants in the adsorbed state on the ice surface, and their stabilization in this state has not been studied to date. In the present work, we report results of experiments with O_3 and H_2O codeposited at 80 K combined with UV irradiation at the wavelengths 250 and 320 nm with emphasis on the attempt to form and observe by FTIR spectroscopy the possible reactive species on the ice surface. Although the experimental temperature is far below typical atmospheric conditions, we performed this study to investigate fundamental processes of the photolysis of adsorbed O_3. In order to rationalize the observed results and to obtain theoretical estimates of the adsorption energy and the key spectral features of

 DOI: 10.1039/b208256j

various surface superoxidants, the quantum chemical modelling of the surface coordination modes of these molecules was carried out.

Experimental and computational details

Processes taking place on the ice surface were studied by means of RA-FTIR spectroscopy. For this purpose, mixtures of ozone, water vapor and argon in various compositions were deposited at a gold-coated copper substrate maintained at 14 K by means of a closed cycle helium cryostat (ROK 10-300, Leybold AG). The rate of the deposition was in the range of 2–5 mmol h^{-1}. The ice film samples were prepared with a typical thickness in the order of 1 μm. Argon was used to make the films more porous by increasing the surface area of the ice. The typical ratio of the components $H_2O/O_3/Ar$ was 1:1:30 with the absolute amounts of H_2O and O_3 in the range of 0.01–0.02 mmol. After annealing to 80 K and evaporation of argon, the O_3–H_2O films were irradiated by a 450 W UV high pressure Hg–Xe lamp (UHM-502 MD, Ushio) using 250 and 320 nm light filters. A liquid water filter (50 mm length) was installed to reduce IR radiation emitted from the arc lamp. The experimental set-up with a 90° mirror in front of the lamp housing allowed the irradiation without changing the optical alignment of the cryostat coupled to the spectrometer. That was especially important for the reproducible irradiation conditions. No temperature increase has been observed during the photolysis experiments. Without any decrease of the ice film thickness during irradiation a complete photolysis of O_3 molecules either sticking on the surface or trapped in the ice was observed. The RA-FTIR spectra of the films were recorded for the source and irradiated mixtures using a Bruker IFS-66v FTIR spectrometer at a resolution of 1 cm^{-1}.

The quantum chemical study was carried out using the density functional theory. The GAMESS(US)[12] program was used for the optimization and frequency calculations of the ice clusters at the B3LYP/6-31++G(d,p) level (UB3LYP for open-shell systems). Some single points calculations were carried out at the B3LYP/6-311++G(2d,2p) level using both the PC GAMESS[13] and Gaussian98[14] packages. The Cartesian basis functions were used for the cluster calculations using the GAMESS packages whereas the pure spherical functions were used for the Gaussian98 calculations. The basis set superposition error (BSSE) corrections were estimated by the counterpoise method.[15]

The cluster models representing the fragments of the O- and H-terminated surface and the crystalline network of the ice were used for the theoretical study. These models included the clusters of four, six, eight, and nine water molecules corresponding to the different planes of the water ice crystal of hexagonal symmetry (*Ih*). In all crystal models, the orientation of the water molecules was chosen in agreement with the "ice rules". The boundary hydrogen and, in some cases, oxygen atoms of the clusters (marked in the figures with asterisks) were fixed in the crystalline positions whereas the full optimization of molecular geometry was performed for the remaining part of the clusters including the molecules modelling the species adsorbed on the ice surface or embedded inside the ice crystal. The stationary points found in the optimization were characterized by frequency calculations with the same geometry constraints. The scaling factor $k = 0.9501$ was applied for the comparison of calculated frequencies with positions of observed IR bands. The value of the scaling factor was chosen on the basis of comparison between the calculated vibrational frequencies of the binary complexes $H_2O_2{\cdot}H_2O$[16] and $HOO{\cdot}H_2O$[17] with the observed frequencies of these complexes isolated in inert cryogenic matrices.[18,19] To make the comparison between the experimental and calculated spectra easier, the envelopes of the calculated IR spectrum were used. The envelope is a superposition of gaussian functions:

$$I(\nu) = \sum_i I_{0i} \exp\left(-(\nu - k\nu_{0i})^2 \Big/ \sigma\right)$$

Here, I_{0i} are the calculated IR intensities corresponding to the calculated frequencies ν_{0i}. The summation is over all the frequencies of corresponding molecular system. A broadening parameter σ of 80 cm^{-2} was chosen for all bands. For simplicity, only scaled frequencies and spectra are shown in the figures.

Results and discussion

RA-FTIR studies

The RA-FTIR spectrum of O_3–H_2O mixtures deposited at a cold metallic surface at 80 K is shown in Fig. 1, trace *a*. The broad intense bands in the regions 3000–3500, 1300–1700 and 500–1000 cm^{-1} are assigned to water ice. The high-intensity band in the region 3000–3500 cm^{-1} has two maxima at 3175 and 3375 cm^{-1}, which is characteristic for the crystalline state *Ih* of water ice.[3] The low intensity peak at 3685 cm^{-1} corresponds to the vibrations of dangling OH-groups terminating the surface.[3] The frequency of these vibrations is slightly red-shifted in agreement with the physical adsorption of ozone.[3,4] The ice films in our experiments exist mostly in the crystalline state and can be characterized by a well-defined surface. The bands at 701, 1035, 1103 cm^{-1} correspond to the free ozone vibrations and the peaks at 2104 and 2340 cm^{-1} are assigned to the vibrations of CO and CO_2 impurities.

The UV irradiation results in remarkable changes of the ice spectrum (Fig. 1, trace *b*). The peaks of free ozone molecules disappear completely whereas two new bands appear: an intense band at 2860 cm^{-1} and a low-intense broad band at 1450 cm^{-1}. Moreover, a remarkable reshaping of the broad bands 3100–3600 and 500–1000 cm^{-1} takes place. The CO peak disappears completely and the CO_2 peak at 2340.0 cm^{-1} grows and becomes broader. The difference spectrum (Fig. 1, trace *c*) reveals additional low-intensity features at 3100 cm^{-1} and 3500 cm^{-1}, which can not unambiguously be considered as new absorption bands. All these changes take place after both 250 and 320 nm irradiation. In the first case, the spectrum changes much faster.

The subsequent annealing of the irradiated films up to 203.2 K has only a slight effect on the IR spectra (Fig. 2). It results in

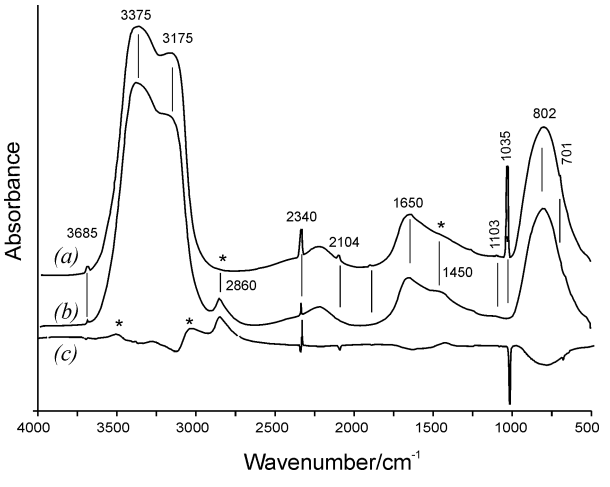

Fig. 1 Experimental IR spectra of the ozone–water ice film before and after UV irradiation. (*a*) spectrum of the source film at 80 K; (*b*) spectrum of the film after irradiation at 320 nm for 10 min; (*c*) difference spectrum.

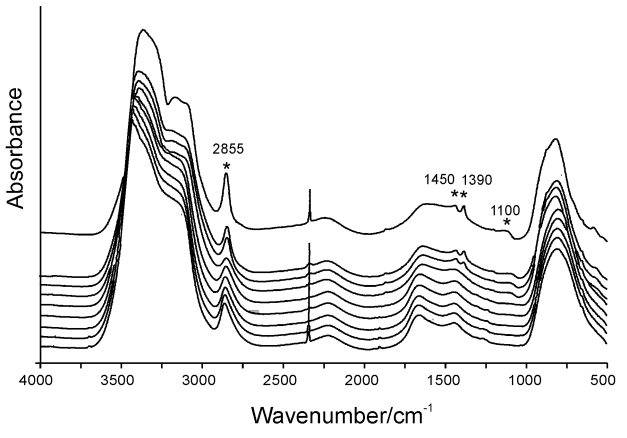

Fig. 2 IR spectra of the UV irradiated ozone–water film recorded during annealing. From bottom to top, the temperature increases from 80 to 203.2 K.

a slight sharpening of the band of 2860 cm^{-1} and shifting it to 2855 cm^{-1} without any changes in the peak intensity. In the case of the band at 1450 cm^{-1}, a low-intensity satellite band at 1390 cm^{-1} appears. In addition, a low-intensity feature appears at 1100 cm^{-1}. The shape of the remaining bands was unchanged indicating that evaporation of the ice occuring during the experiments is negligible. Thus, the reshaping of the ice bands after irradiation is a consequence of changes in the film structure and composition induced by the photolytic reactions. We can conclude on the basis of the character of the observed spectra, that there is no observable evidence of ionic structures formed during the photolysis. The newly observed bands have rather sharp profiles, without very broad maxima which are typical for the ionic interaction in partially disordered media.

The newly observed bands can not be assigned on the basis of the fundamentals of gas-phase H_2O_2, free $HO^{\bullet}$, and $HOO^{\bullet}$ radicals.[20,21] Obviously, the vibrational frequencies of species produced by the photo-induced reactions are strongly influenced by the complex formation with the ice surface or by the environment effects after the incorporation of these molecules into the crystalline network.

Quantum chemical modelling

Photolytic decomposition of ozone in the presence of water in the gas phase is usually represented by a series of reactions:[1]

$$O_3 \rightarrow O_2(a\ ^1\Delta_g) + O(^1D) \quad (1a)$$

$$O_3 \rightarrow O_2(X\ ^3\Sigma_g) + O(^3P) \quad (1b)$$

$$O(^1D) + H_2O \rightarrow HO^{\bullet} + HO^{\bullet} \quad (2)$$

$$HO^{\bullet} + HO^{\bullet} \rightarrow H_2O_2 \quad (3)$$

$$HO^{\bullet} + O(^1D) \rightarrow HOO^{\bullet} \quad (4)$$

Although the quantum yields of the reactions (1a) and (1b) are different at different wavelengths, it is known that both singlet and triplet oxygen atoms can be formed during irradiation at 250 and 320 nm.[1]

The formed species can initiate various secondary processes, for example:

$$HO^{\bullet} + H_2O_2 \rightarrow H_2O + HOO^{\bullet} \quad (5)$$

$$O(^1D) + H_2O_2 \rightarrow HO^{\bullet} + HOO^{\bullet} \quad (6)$$

$$O(^1D) + H_2O \rightarrow H_2O_2 \quad (7)$$

$$O(^3P) + HOO^{\bullet} \rightarrow HO^{\bullet} + O_2 \quad (8)$$

$$HO^{\bullet} + HOO^{\bullet} \rightarrow H_2O + O_2(X\ ^3\Sigma_g) \quad (9)$$

$$O(^1D) + HOO^{\bullet} \rightarrow O_2(a\ ^1\Delta_g) + HO^{\bullet} \quad (10)$$

Thus, the ozone photolysis results in the formation of H_2O_2, which is the most stable product, proceeding through the formation of singlet and triplet oxygen atoms, singlet and triplet oxygen molecules, $HO^{\bullet}$ and $HOO^{\bullet}$ radicals.

H_2O_2 adsorption modes on the ice surface. H_2O_2 molecules formed in the photolysis can interact with the ice surface in different coordination modes. It can form the one-, two-, or multi-fold coordination complexes with the dangling OH groups or terminal oxygen atoms at the basal or side planes of the ice crystal distinguished in both energy and vibrational frequencies.

The optimized structure of the one-fold coordination adsorption complex of H_2O_2 (**I**) is shown in Fig. 3*a*. The binding energy and the values corrected by the basis set superposition error (BSSE) and zero point energy (ZPE) are given in Table 1. The interaction of H_2O_2 with a terminal O atom is similar to the most stable conformation of a binary complex[18] between H_2O and H_2O_2 both in structure and in energy. The calculated adsorption energies are listed in Table 1. The energy of this coordination (−36.0 kJ mol^{-1}) is close to the binary complex value at the B3LYP/6-31++G(d,p) level (−32.2 kJ mol^{-1}). The frequency calculation shows that the frequency of the lowest OH stretching mode (stretching of OH group of coordinated H_2O_2 molecule) is 3448 cm^{-1}. The scaled value is 3276 cm^{-1}, which is far from the observed band of 2860 cm^{-1}.

The one-fold coordination of H_2O_2 molecule at the dangling hydrogen site (*i.e.* coordination of $HOHO\cdots H{-}O_{ice}$ type) is not favorable. The optimization of the corresponding structure results in the reorientation of H_2O_2 with the formation of an additional hydrogen bond with boundary atoms.

A two-fold coordination complex at the side crystal plane can be formed with two neighbouring dangling oxygen atoms (**IIa**, Fig. 3*b*) or one neighbouring dangling OH group and dangling O atom (**IIb**, Fig. 3*c*). In both cases, the coordination of H_2O_2 does not break the $O{-}H\cdots O$ surface hydrogen bond. Moreover, the H_2O_2 adsorption is even strengthening the hydrogen bond, acting like an additional bridge between two centers and decreasing the O–O distance. It results in an increase of the frequency of O–H vibrations of surface groups. The frequencies of the H_2O_2 molecule are decreased. The lowest value of the OH stretching frequency is 3480 cm^{-1} (OH group of H_2O_2 molecule) for **IIa**, and 3484 cm^{-1} for **IIb**. The coordination energies corrected with BSSE and ZPE for these models (Table 1) are close (−27.2 and −25.9 kJ mol^{-1}) and practically the same as in the case of the one-fold coordinated model (−26.8 kJ mol^{-1}).

The interaction of the H_2O_2 molecule with the basal plane of the ice *Ih* crystal surface was modelled with a cluster of nine water molecules. The H_2O_2 molecule was initially located close to two dangling O sites and the geometry optimization of this structure was performed. During the optimization, the initial orientation of H_2O_2 molecule was only slightly distorted. The optimized structure (**III**) is shown in Fig. 3*d*. This shows the formation of multiple hydrogen bonds (judging by the interatomic distances between O and H atoms). The coordination energy is shown in Table 1 with the final corrected value of −28.5 kJ mol^{-1}. The frequency calculation shows that two vibrations have strongly red-shifted frequencies of 3316 and 3374 cm^{-1} (scaled frequencies are 3150 and 3205 cm^{-1}). Apart from these bands, there are two vibrations in the region 3400–3500 cm^{-1} and the remaining OH valence modes are located in region the 3500–3750 cm^{-1}. The vibration mode 3374 cm^{-1}

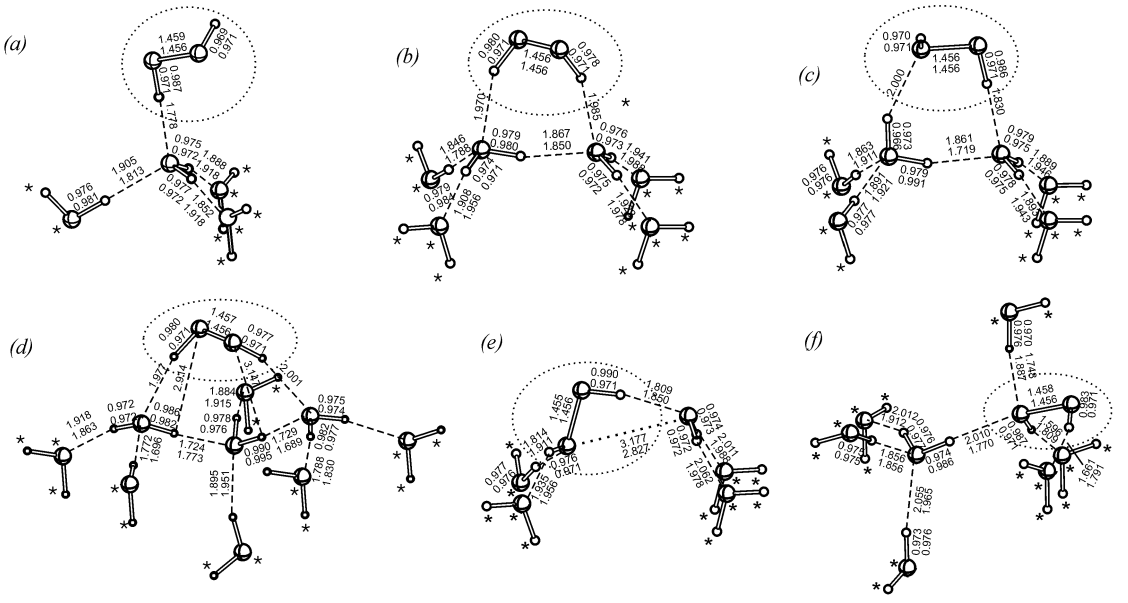

Fig. 3 The optimized structures and key geometry parameters of the adsorption complex between ice clusters and H_2O_2 molecules for different coordination modes (bond lengths in Å). Bottom values—source cluster, upper values—complex with H_2O_2. Asterisks mark the atoms fixed during the optimisation. Dashed line marks the H_2O_2 molecule.

has a large admixture of boundary OH groups whereas the frequency 3316 cm^{-1} is practically completely assigned to the OH-stretching of a central unfixed H_2O molecule between two dangling oxygens where the H_2O_2 molecule is coordinated. However, the lowest fundamental frequency (scaled value of 3150 cm^{-1}) is far from the observed band of 2860 cm^{-1}.

It should be noted that the transition from the minimal cluster **I** to the largest system **III** results in changes of only 20% of the binding energy, whereas the difference of the binding energies between clusters **IIa**,**b** and **III** is only 5–10%. Thus, we expect that the increase of the binding energy due to the transition from the system **III** to the larger clusters will probably be smaller than 10%.

Inclusion of H_2O_2 molecules into the crystalline network. The H_2O_2 molecule formed (at the last end) in the ozone photolysis can be built-in into the ice crystal. The optimized structures for clusters **II** and **IV** representing the different modes of coordination are shown in Fig. 3*e*,*f*. The H_2O_2 molecule forms three or four hydrogen bonds with neighbouring water molecules. The corresponding optimized energies of the clusters and the energies of inclusion (estimated as an energy of reaction of substitution of one of H_2O molecules in the cluster by molecule H_2O_2) are presented in Table 2. The ZPE corrected energies of inclusion have small positive values demonstrating that hydrogen bonds between H_2O_2 and the crystalline network are relatively weak and can not compensate the energy of the structural distortion. As a consequence, the calculated vibrational frequencies of both structures are only slightly distorted in comparison with the free H_2O_2 molecule. The lowest OH-stretching frequencies are 3401 cm^{-1} (OH stretch of H_2O_2, scaled value 3230 cm^{-1}) and 3507 cm^{-1} (OH-stretch of boundary H_2O molecules, scaled value 3332 cm^{-1}).

The vibrational bands of H_2O_2 on the ice surface and inside the ice crystal. On the basis of the results above, we conclude that the calculated OH vibration fundamentals of the H_2O_2 molecule adsorbed on the surface or incorporated into the ice network are situated in the region 3200–3400 cm^{-1}, far from the observed position 2860 cm^{-1}. The vibrations of the water molecules involved in the interaction with H_2O_2 are also situated higher than 3100 cm^{-1} and, thus, can not explain the appearance of the intense band at 2860 cm^{-1}. Two physical effects can, in principle, affect the valence vibrations resulting

Table 1 Adsorption energies (ΔE_{tot}) of H_2O_2, $HO^{\bullet}$, and $HOO^{\bullet}$ on the ice surface calculated for the different modes of coordination at the B3LYP/6-311++G(2d,2p)//B3LYP/6-31++G(d,p) and B3LYP/6-31+(d,p) levels (in parentheses)

Cluster model	Type of coordination	E_{tot}[a]/E_h	ΔE_{tot}/kJ mol^{-1}	ΔE_{tot} + BSSE[b] /kJ mol^{-1}	ΔE_{tot} + BSSE + ZPE[c] /kJ mol^{-1}
H_2O_2 on the ice surface					
I, Fig. 3a	$HOOH\cdots O_{ice}$	−457.334538	−32.2 (−36.0)	−29.7 (−32.6)	−24.3 (−26.8)
IIa, Fig. 3b	$O_{ice}\cdots HOOH\cdots O_{ice}$	−609.931749	−38.1 (−42.3)	−34.3 (−36.8)	−25.1 (−27.2)
IIb, Fig. 3c	$H_{ice}\cdots OHOH\cdots O_{ice}$	−609.934587	−36.0 (−41.0)	−32.6 (−35.6)	−23.4 (−25.9)
III, Fig. 3d	*Multiple H-bonds*	−839.155103	−40.2 (−44.4)	−36.0 (−38.5)	−28.5 (−31.0)
$HO^{\bullet}$ on the ice surface					
IIa, Fig. 8a	$^{\bullet}OH\cdots O_{ice}$	−534.143144	−30.1 (−33.5)	−28.0 (−30.1)	−17.6 (−19.7)
IIb, Fig. 8b	$HO^{\bullet}\cdots H\text{–}O_{ice}$	−534.135802	−7.5 (−9.2)	−6.7 (−7.5)	−0.4 (−1.3)
$HOO^{\bullet}$ on the ice surface					
IIa, Fig. 10a	$^{\bullet}OOH\cdots OH_{ice}$	−609.297169	−48.5 (−54.4)	−46.0 (−50.2)	−37.2 (−41.4)
IIb, Fig. 10b	$H_{ice}\cdots{}^{\bullet}OOH\cdots O_{ice}$	−609.585236	−45.2 (−49.4)	−41.8 (−43.9)	−31.4 (−33.5)

[a] Total energy of optimized structure obtained at the B3LYP/6-31++G(d,p) level (GAMESS(US)). [b] Adsorption energy corrected by the basis set superposition error (BSSE). [c] Adsorption energy corrected by BSSE and zero point energy (ZPE).

Table 2 Energies of inclusion of H_2O_2 into the ice crystal calculated at the B3LYP/6-31+G(d,p) level

Cluster model	E_{tot},[a] / E_h	ΔE_{tot}[b] / kJ mol^{-1}	ΔE_{tot} + ZPE[c] / kJ mol^{-1}
IV, Fig. 3e	−686.325208	27.6	24.3
IIa, Fig. 3d	−533.519798	−2.1	17.2

[a] Total energy of optimized structure obtained at the B3LYP/6-31++G(d,p) level. [b] Energy of substitution reaction [Ice cluster] + H_2O_2 → [Ice cluster with H_2O_2] + H_2O. [c] Energy of inclusion corrected by zero point energy (ZPE).

in the appearing of the vibration bands in low-frequency region: (i) an effect of the surface electrostatic field and (ii) increasing the intensity of combination bands of the H_2O_2 molecule due to environmental effects.

In order to take into account the first effect, we repeated the calculations of H_2O_2 adsorbed at the basal plane of the ice crystal (**III**) with an electrostatic field imposed in the normal direction to the surface. The magnitude of the field was chosen to be 0.01 E_h (about 5×10^9 V m^{-1}) which is close to the mean value of different experimental and theoretical estimations ranging from 0.3×10^9 to 7×10^9 V m^{-1}.[2] The optimization of the molecular geometry of cluster **III** was repeated starting from the optimal geometry obtained without the field. The final structure was only slightly different from the initial structure. In contrast to recent results,[22] the frequency calculation performed shows that an additional electrostatic field also only has a slight effect on the frequencies of both adsorbed molecules and the surface groups of cluster **III**. Although the sign of the frequency shift was correct (blue shift for the frequencies of dangling OH groups and red shift for the adsorbed H_2O_2), the magnitude of the frequency changes was typically less than 100 cm^{-1}. The maximum changes were related to the high-frequency vibrations of the internal OH fragments (with dipole moments parallel to the electric-field vector) whereas the lowest frequencies of the surface groups (with dipole moments directed parallel to the surface plane) were practically not changed and located in the region 3100–3200 cm^{-1}. Thus, we conclude that the band at 2860 cm^{-1} observed experimentally can not be explained by the H_2O_2 fundamentals shifted due to the crystal field effects.

The calculation of combination band intensities is still not a commonly-used procedure in practice of applied computational chemistry. Therefore, the intensity of combination bands of H_2O_2 was estimated on the basis of the analysis of the IR spectra of the binary complexes. For this purpose, the frequencies of some binary complexes of hydrogen peroxide and related molecules with electron donors, namely $H_2O_2{\cdot}H_2O$,[18] $H_2O_2{\cdot}H_2O_2$,[19] $H_2O_2{\cdot}CO$,[23] $H_2O_2{\cdot}NH_3$,[24] $HOO{\cdot}H_2O$,[25] isolated in inert low-temperature matrices were inspected. Two of them, ($H_2O_2{\cdot}H_2O_2$, $H_2O_2{\cdot}CO$) exhibit bands in the region 2700–2900 cm^{-1}. These bands are assigned to the combination band $\nu_2 + \nu_6$ of the H_2O_2 molecule.[19,23] Although the intensity of this band in the gas phase is low, it might be higher in a coordinated state. For example, the intensity of this band in the isolated complex $H_2O_2{\cdot}NH_3$ is comparable with the OH band intensity (about 100 km mol^{-1}). Therefore, we modelled the spectrum of adsorbed H_2O_2 molecule using the calculated (B3LYP/6-31++G(d,p)) frequency of $\nu_2 + \nu_6$ and used the value 100 km mol^{-1} for its intensity.

Fig. 4*a*,*b* show the IR spectrum of hydrogen peroxide molecule adsorbed on the basal plane of the ice surface (cluster **III**). The changes in the calculated band position due to the electrostatic field imposed to cluster **III** are shown with dashed trace in Fig. 4*b*. The asterisk marks the calculated position of the combination band. The comparison between the experimental (Fig. 1) and calculated spectrum demonstrates that the proposal about the combination character of the band 2860 cm^{-1} is in agreement with experimental results (the calculated position of the $\nu_2 + \nu_6$ band 2898 cm^{-1}, scaled value 2753 cm^{-1}). Moreover, the calculated OH band of the ice is reshaped in a similar manner as it is for the observed one. We conclude that this reshaping is a consequence of the admixture of H_2O_2 fundamentals with the IR intensities, which are different from those of water molecules of the ice. Similarly, Fig. 4*c* and *d* show the

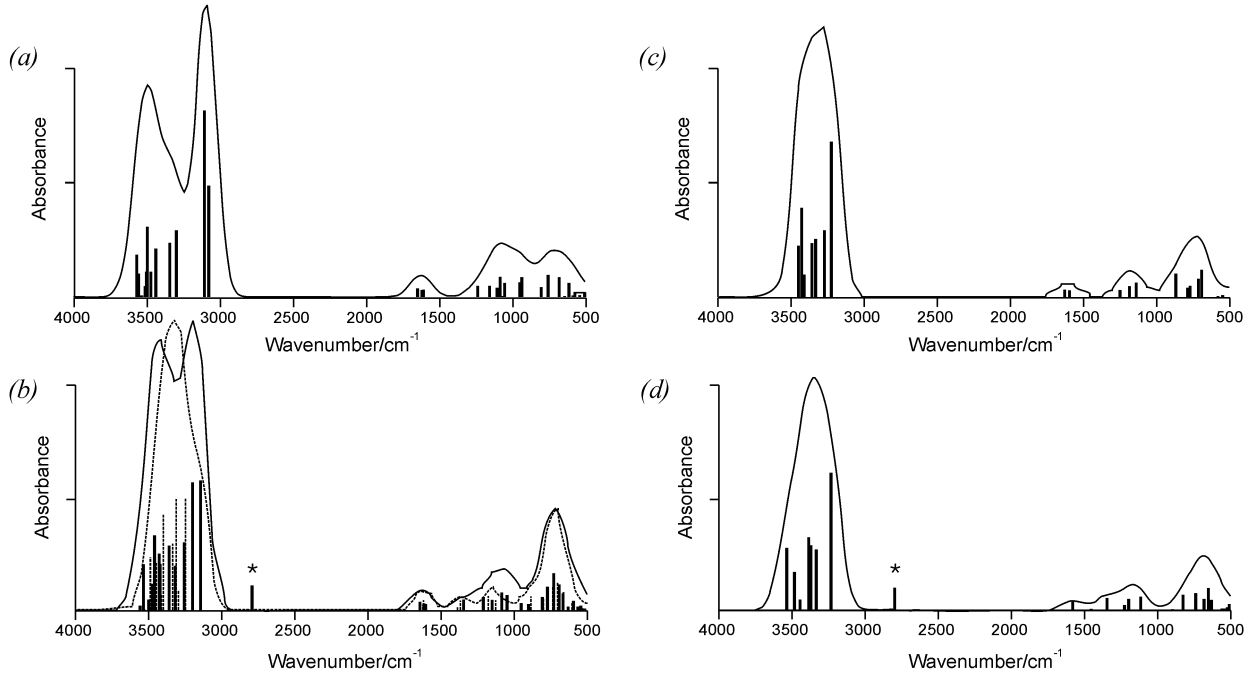

Fig. 4 The calculated IR spectra of H_2O_2 adsorbed on the ice surface and incorporated into the crystalline network. (*a*) Spectrum of source cluster **III**; (*b*) spectrum of cluster **III** with adsorbed H_2O_2 (dashed trace shows the effect of external electrostatic field); (*c*) spectrum of source cluster **IV**; (*d*) spectrum of cluster **IV** with incorporated H_2O_2. Asterisks mark position of $\nu_2 + \nu_6$ band of H_2O_2.

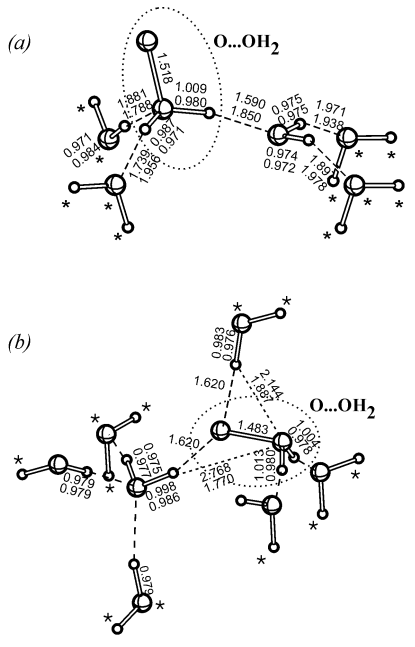

Fig. 5 The optimized structure of the ice clusters after inclusion of $O(^1D)$ atom into the crystalline network. (*a*) the structure of cluster **II** with $O(^1D)$ forming the oxywater complex on the ice surface; (*b*) cluster **IV** with $O(^1D)$ forming the oxywater complex inside the ice.

calculated frequencies of the H_2O_2 molecule incorporated in the ice network which is also close to the experimental spectrum.

Interaction of $O(^1D)$ with the ice crystalline network. The key step of the ice surface photolysis is an interaction of $O(^1D)$ with the surface molecules. This process was modelled by arranging the oxygen atom close to the surface of cluster **IIa**, and in the space inside the water cluster of eight water molecules (**IV**) representing the ice crystalline network. The initial position ensured that the distances between the nearest atoms were about 1.2 Å (O–O) and 1.5 Å (H–O). The following geometry optimization shows that $O(^1D)$ does not break the O–H bonds (as it is expected for the gas-phase reactions). Instead, the energetically very profitable complex with one of the internal H_2O molecules (unfixed in this model) with an O···O distance of about 1.5 Å and a valence angle HOH of about 116° was formed. The key geometry parameters of the optimized structures are shown in Fig. 5. The geometry of the complex corresponds to the oxywater structure $O\cdots OH_2$ forming four additional hydrogen bonds with neighbouring water molecules. The energies of the $O(^1D)$ complex formation for the different models calculated at the B3LYP/6-31G++G(d,p) level are shown in Table 3. During another experiment we stretched the O–H band of the water molecule (in cluster **IV**) adjacent to the one-fold coordinated O atom of the complex to form a pair of HO•. However, the O atom was returning to the initial position during the subsequent optimization. Thus, the formation of the HO• pair from the $O\cdots OH$ complex stabilized by the crystalline environment was not energetically profitable.

This result is a remarkable fact regarding the possibility of the experimental observation of oxywater.[26] On the basis of these results, one can conclude that the crystalline network of ice can have a crucial effect on the stability of the oxywater complex. The four additional hydrogen bonds formed with the neighbouring water molecules in cluster **IV** decrease the energy of the oxywater structure to 110.9 kJ mol^{-1} (relatively to H_2O_2 inside the ice) whereas the gas-phase energy (relatively to free H_2O_2 molecule) is 191.6 kJ mol^{-1} (G2 calculation) and 189.1 kJ mol^{-1} (B3LYP/6-31+G(2d,2p)).[27] The recent study of the environmental effect of the liquid water on the kinetic barrier of the oxywater formation from H_2O_2 gave a similar result, decreasing the activation energy from 221.3 kJ mol^{-1} to about 123.4 kJ mol^{-1}.[28]

The possible way of destruction of the oxywater structure is a rearrangement to H_2O_2 . The moving of the H atom close to the one-fold coordinated O atom results in the system rearrangement with the formation of H_2O_2 built-in into the ice crystalline network. The activation barrier of this process was found to be 8.5 kJ mol^{-1} for the structure shown in Fig. 5*a* whereas the barrier of 70.2 kJ mol^{-1} was found for the structure in Fig. 5*b*. The explanation of the large difference between two structures is a existence of additional hydrogen bonds inside the ice cluster **IV**. In the case of cluster **IIa**, the HOO moiety undergoes the reorientation resulting in the strong reconstruction of the cluster. The optimized structure of the transition state **TS1** for this reaction is shown in Fig. 6*a*. In the case of cluster **IV**, the reorientation of HOO is impossible because of the additional hydrogen bonds formed with the neighbouring water molecules. Thus, the corresponding transition state **TS2** (Fig. 6*b*) is close to the initial structure of the complex. The energetic and thermodynamic parameters of the located transition states are presented in Table 4. The values of the calculated activation barriers for **TS2** are much higher than for the gas-phase conditions.[28] Earlier, the low activation barrier in the gas phase (16.3 kJ mol^{-1}, G2 calculation[28]) and relatively high exothermicity of the rearrangement of the oxywater complex explained why this structure was not observed in the matrix isolation experiments.[10] However, as it is evident from the present calculations, the situation may be different in a solid medium which can form the multiple hydrogen bonds with the oxygen atom stabilizing the oxywater complex. The calculations show that, although the complex of $O(^1D)$ is unstable at the ice surface, it can be stabilized by the multiple hydrogen bonds inside the ice crystal as it is shown in Fig. 5*b*. On the basis of these facts, we can propose that attempts to observe the oxywater or related complexes should be concentrated, probably, on solid state observations of oxygen-containing molecules having bulky substituents and the ability to form hydrogen bonds with the substrate.

The calculated spectra of the oxywater structures formed at the ice surface and embedded into the crystalline network are shown in Fig. 7*a*,*b*. The frequency calculation for the structure $O\cdots OH_2$ inside the ice results in two extremely low values of

Table 3 Energies of oxywater formation from $O(^1D)$ and ice (ΔE_1) and from H_2O_2 inside the ice (ΔE_2) calculated at the B3LYP/6-31+G(d,p) and G2 (in parentheses) levels

Model	Type of coordination	E_{tot}[a]/E_h	ΔE_1/kJ mol^{-1}	ΔE_1 + ZPE/kJ mol^{-1}	ΔE_2/kJ mol^{-1}	ΔE_2 + ZPE/kJ mol^{-1}
Free molecules $H_2O + O(^1D)$	$O\cdots OH_2$ (gas phase)	−151.418871	−224.3 (−149.4)	−211.3 (−144.3)	190.4 (191.6)	177.0 (191.6)
IIa, Fig. 6*a*	$O\cdots OH_2$ (surface layer)	−533.462296	−265.7 (−190.8)[b]	−259.8 (−192.9)[b]	151.0	127.2
IV, Fig. 6*b*	$O\cdots OH_2$ (inside crystal)	−686.282905	−275.7 (−200.8)[b]	−272.0 (−205.0)[b]	110.9	108.4

[a] Total energy of optimized structure obtained at the B3LYP/6-31++G(d,p) level (GAMESS(US)). [b] Values obtained by correction of corresponding value ΔE_1(B3LYP) by the difference between G2 and B3LYP results for the gas phase model ΔE_1(G2) − ΔE_1(B3LYP).

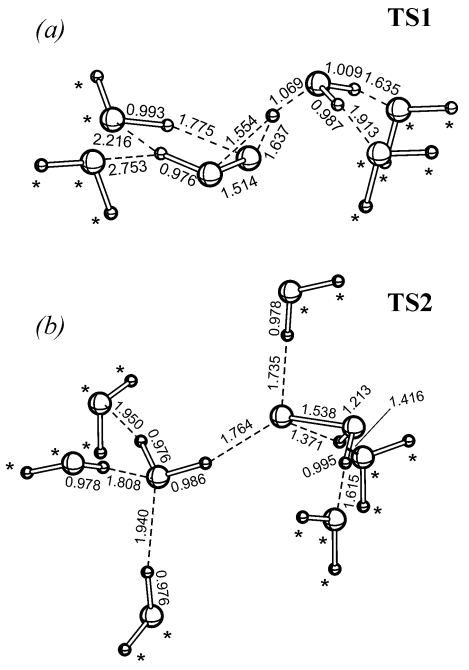

Fig. 6 The located structures of transition states for the rearrangement of the oxywater complex to H_2O_2. (*a*) oxywater complex on the ice surface; (*b*) oxywater complex inside the ice.

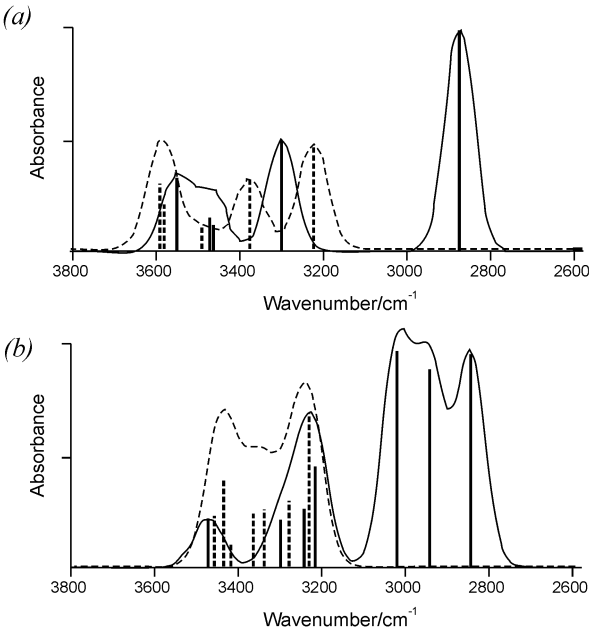

Fig. 7 The calculated IR spectrum of the ice crystal after inclusion of singlet oxygen atom into the crystalline network. (*a*) oxywater complex on the ice surface; (*b*) oxywater complex inside the ice. Dashed trace and bars—source cluster, solid—cluster after inclusion of $O(^1D)$.

2992 and 3095 cm^{-1} (scaled values 2842 and 2940 cm^{-1}) of high intensity OH vibrations of H_2O in the $O\cdots OH_2$ complex and the free H_2O molecule coordinated with $O\cdots OH_2$. It should be noted that the calculated frequency 2842 cm^{-1} is located in the region of the observed band at 2860 cm^{-1}. Thus, the calculated IR bands of the oxywater complex formed by the coordination of $O(^1D)$ on the ice surface are located in the region of the experimentally observed band at 2860 cm^{-1} and are close to the position of $\nu_2+\nu_6$ band of adsorbed H_2O_2. Among the low-frequency vibrations of this complex, the O–O stretching mode (778 cm^{-1}) has a low intensity (1.8 km mol^{-1}) and obviously is hidden by non-transparent region of the ice. The calculated frequencies of bending modes are located in region 1600–1690 cm^{-1} and are close to the frequencies of H_2O_2. Thus, we can not unambiguously determine whether this structure exists on the surface on the basis of present experimental results. Because $O(^1D)$ is strongly quenched by the water molecules in the gas phase, we hardly expect that the molecular pathway including the oxywater formation on the ice will be predominant. However, the facts of crucial stabilization of this structure due to the environmental effects are evident that it can be possible.

Interaction of $O(^3P)$ atoms with the ice crystalline network. In contrast with $O(^1D)$, it was found that the triplet oxygen atom $O(^3P)$ arranged in the ice crystalline network (modelled by cluster **IV**) does not react with neighbouring molecules. $O(^3P)$ also does not break the hydrogen bonds of the ice crystal. During the geometry optimization it moves away from the oxygen atoms of the water molecules, taking the positions inside the void region of the crystal and forming a structure similar to the weak complex $O\cdots H$–OH with a coordinated water molecule. The energy of the optimized structure has a positive value of +34.7 kJ mol^{-1}, probably because of a weak $O\cdots H$ bonding and strong repulsion from the surrounding molecules. The formation of a weak complex of triplet oxygen with ice is in agreement with the results of Pehkonen *et al.*,[29] who observed a weakly bound complex $HOH\cdots O(^3P)$ in argon matrix.

Table 4 Calculated parameters of the transition states for the rearrangement of oxywater complex to H_2O_2 at the ice (B3LYP/6-31+G(d,p))

Transition state	ν_{im}[a] / cm^{-1}	E_{tot}[b] / E_h	E_a[c] / kJ mol^{-1}	E_a + ZPE[d] / kJ mol^{-1}
TS1	733*i*	−533.459085	8.5	0.2
TS2	1556*i*	−686.256185	70.2	53.1

[a] Imaginary frequency of transition state. [b] Total energy of optimized structure. [c] Activation energy. [d] Activation energy corrected by zero point energy.

Interaction of singlet and triplet oxygen molecules with the ice crystalline network. Singlet and triplet oxygen molecules placed inside the ice crystal tend to move outside the cluster representing the ice structure. No complex structures or hydrogen bonds were found for the singlet and triplet states of the oxygen molecule. We conclude that the oxygen molecules are only physically adsorbed at the ice crystal surface.

Interaction of the HO• radical with the ice surface. It is believed that HO• can interact with dangling hydrogen and oxygen atoms or the surface (in-plane) hydrogen bonds O–$H\cdots O$. In the last case, HO• are expected either to form an additional hydrogen bond with a bridging H atom or to insert into the hydrogen bond forming the quasi-cyclic surface structure –O–$H\cdots$O–$H\cdots$O–. These kinds of interactions were modelled using the clusters **II** similar to ones shown in Fig. 3*b*,*c*. HO• was initially located over the surface oxygen, over the terminal hydrogen atoms, over the H atom forming the hydrogen bond (HO• is oriented in perpendicular direction to the surface plane), or over the $H\cdots O$ fragment (in parallel direction). The subsequent optimization started from these initial geometries and resulted in only two stable structures with one-fold HO• coordination on the terminal O or H atoms. Thus, the adsorption of HO• causing the rupture of a surface H-bond is unfavorable. The optimized structures of the located complexes are shown in Fig. 8. The corresponding binding energies are given in Table 1. The most favorable complex

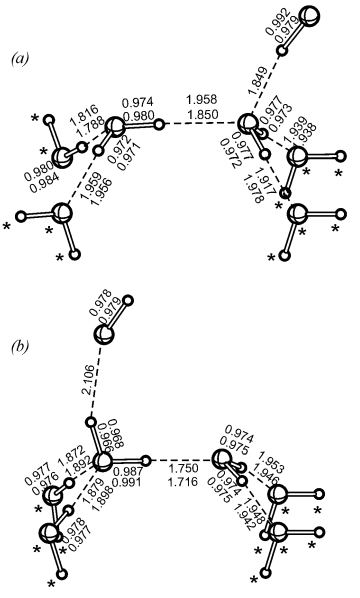

Fig. 8 The optimized structure and key geometry parameters of HO• adsorbed on the ice surface for two coordination modes (*a*) coordination on the terminal oxygen atom; (*b*) coordination on dangling H atom (bond lengths in Å). Bottom values—source cluster, upper values—cluster with adsorbed HO• radical.

(dangling-O coordinated) has a final energy slightly different from the binary complex $H_2O{\cdot}HO^{\bullet}$ (-19.7 kJ mol^{-1}). The OH bond in this complex is remarkably elongated: r(O–H) = 0.990 Å (0.979 Å in isolated radical). However, the calculated vibrational frequencies (Fig. 9) are quite close to the frequencies of the initial cluster. It should be noted, that the vibration of the OH bond of the radical is located in the region of 3400–3500 cm^{-1}, in the middle of the OH band of the cluster. The lowest frequency values are assigned to the vibrations of surface water molecules and located at about 3200 cm^{-1}.

Interaction of the HOO• radicals with the ice surface. Like HO•, HOO• coordination modes were studied using the

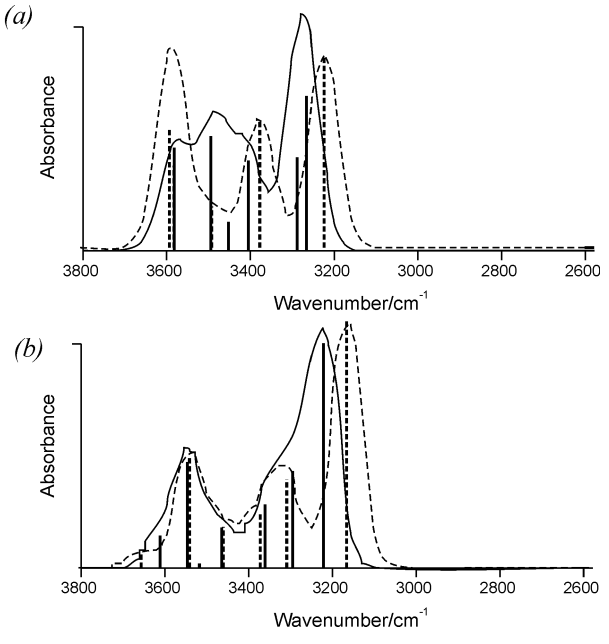

Fig. 9 The calculated IR spectra of the ice surface due to the adsorption of HO• radical. (*a*) adsorption on the terminal oxygen atom; (*b*) adsorption on the terminal hydrogen atom. The dashed trace and bars—source cluster, solid—cluster with adsorbed OH radical.

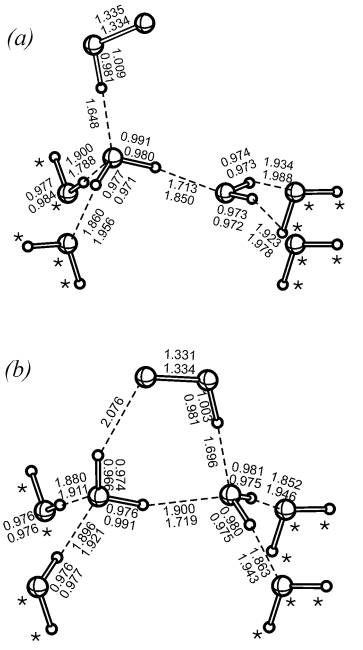

Fig. 10 The optimized structure and key geometry parameters of HOO• radical adsorbed on the ice surface for two coordination modes (bond lengths in Å). (*a*) Coordination on the terminal oxygen and surface hydrogen atoms; (*b*) coordination on terminal oxygen and dangling hydrogen atoms. Bottom values—source cluster, upper values—cluster with adsorbed HOO•.

clusters **II**. The HOO• was placed near to the O–H···O surface hydrogen bond to form the bridge-like structure between H and O atoms. The subsequent geometry optimization of the cluster shows that the HOO• radical does not break the surface hydrogen bond. It can only form the one-fold coordinated complexes with both kinds of the surface bond oxygens. The O···HOO• complex with a terminal oxygen has a binding energy of -33.9 kJ mol^{-1}. The HOO• moiety is twisted relatively to the surface hydrogen bond direction (the dihedral angle is about 60°). The more stable structure is formed when the HOO• radical reacts with the opposite O atom of the surface hydrogen bond. The optimized geometry of this complex is shown in Fig. 10*a*. The structure of the complex is not twisted because of the additional coordination of the OO• moiety at the H atom of the O–H surface group. The binding energy of this complex is -54.3 kJ mol^{-1}. The r(O–H) distance of coordinated peroxy radical is sufficiently increased compared to the free molecule: r(OH) = 1.009 Å (0.981 Å in the isolated HOO•). It results in the significant decrease of the frequency of the OH group valence vibration of the adsorbed HOO• radical to 3105 cm^{-1} (scaled value 2950 cm^{-1}) whereas the frequency of the isolated molecule is 3574 cm^{-1} (scaled 3395 cm^{-1}). The calculated IR spectrum of the HOO• bound to the ice surface is shown in Fig. 11. We conclude that the calculated position of the intense peak of HOO• adsorbed on the surface (2950 cm^{-1}) is only 90 cm^{-1} higher than the position of the observed intense band of 2860 cm^{-1}. Thus, the experimental band (assigned to $\nu_2 + \nu_6$) probably contains the admixture of OH stretching of HOO•. An additional argument for this is the shift of the band 2860 cm^{-1} to 2855 cm^{-1} due to the annealing which results in the destruction of HOO• when the temperature increases.

Conclusions

The recorded IR spectra of the ozone–water films deposited at a cold metallic surface at 80 K demonstrate that a new sharp intense band at 2860 cm^{-1} and a low-intense band at 1450

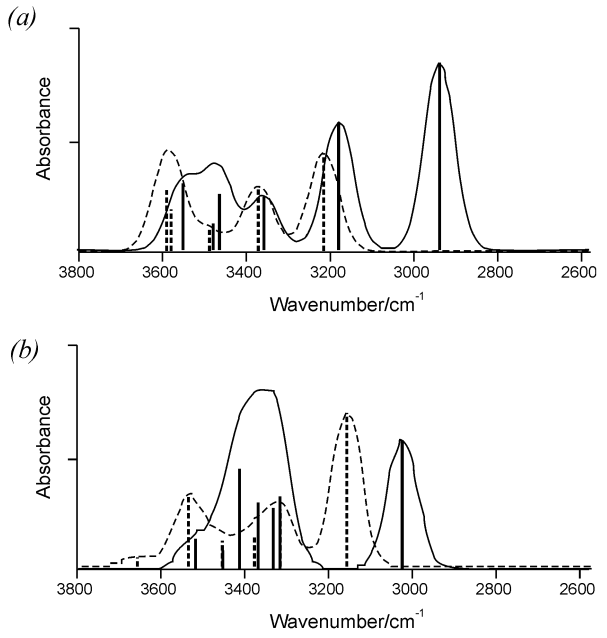

Fig. 11 The calculated IR spectra of the ice surface due to the adsorption of HOO•. (*a*) The coordination on the terminal oxygen and surface hydrogen atoms; (*b*) coordination on the terminal oxygen and dangling hydrogen atoms. Dashed trace and bars—source cluster, solid—cluster with adsorbed HOO•.

cm^{-1} appear after irradiation with UV light together with the remarkable reshaping of crystalline ice bands in regions 3100–3600 cm^{-1} and 500–1000 cm^{-1}. The annealing of irradiated films has only a slight effect on the intensity of new bands making the band of 2860 cm^{-1} sharper and causes the appearance of low-intense band at 1390 cm^{-1}.

The quantum chemical study shows that among the atoms and molecules which can be formed in the ozone photolysis ($O(^1D)$, $O(^3P)$, $O_2(a\ ^1\Delta_g)$, $O_2(X\ ^3\Sigma_g)$, HO•, HOO•, and H_2O_2), the species $O(^3P)$, $O_2(a\ ^1\Delta_g)$, and $O_2(X\ ^3\Sigma_g)$ interact with the ice surface only weakly with energies typical to physical adsorption. In contrast, HO•, H_2O_2, and HOO•, form hydrogen bound complexes with estimated binding energies of −17.6, −28.5, and −37.2 kJ mol^{-1}, respectively. The singlet oxygen atom is able to strongly interact with the ice crystal with binding energy up to −200.8 kJ mol^{-1}. The coordination of $O(^1D)$ results in the formation of the complex inside the ice crystalline network of the oxywater structure $O\cdots OH_2$ stabilized by additional hydrogen bonds with neighbouring water molecules. This stabilization corresponds to the significant decrease of energy of oxywater formation (relatively to H_2O_2) up to 108.4 kJ mol^{-1} in comparison with 190.4 kJ mol^{-1} in the gas phase. This allows consideration of the $O(^1D)$ complex stabilized by hydrogen bonds as possible intermediate of ozone photolysis occurring on the ice surface.

Among the considered molecules, several species absorb in the region 2700–2900 cm^{-1}: H_2O_2 ($\nu_2+\nu_6$ combination band), HOO• coordinated on the terminal oxygen of the ice, and the $O(^1D)$ complex both inside the ice crystal and on the ice surface. The IR bands of the adsorbed HO• coincide with non-transparent region of the ice crystal and can not be observed by IR spectroscopy. It is important to note that no fundamentals of adsorbed H_2O_2 was found to be located lower than 3200 cm^{-1} which correlates well with the medium value of binding energy. Thus, the band of 2860 cm^{-1} can not be explained by the OH-vibrations of H_2O_2 shifted due to the adsorption. The present experiments did not allow unambiguously determination as to whether the 2860 cm^{-1} is assigned only to H_2O_2 (which is formed in the ozone photolysis as a basic product) or also has admixture of the IR bands of other species (*e.g.* $O(^1D)$ or HOO• complexes as this is predicted by the theory). This assignment will be checked by additional experiments with isotopic species and further variation of experimental conditions combined with quantum chemical modelling. Such studies are the subject of our further work.

Acknowledgements

This work was partially supported by the Russian Foundation for Basic Research (Project No. 00-03-32094). S.I. and P.S. thank the Alfred-Wegener Institute for fellowship support during the course of the work.

References

1 P. Wayne, *Chemistry of Atmospheres*, Oxford University Press, Oxford, 2001.
2 C. Girardet and C. Toubin, *Surf. Sci. Rep.*, 2001, **44**, 159–238.
3 H. Chaabouni, L. Schriver-Mazzuoli and A. Schriver, *J. Phys. Chem. A*, 2000, **104**, 6962–6969.
4 F. Borget, T. Chiavassa, A. Allouche and J. P. Aycard, *J. Phys. Chem. B*, 2001, **105**, 449–454.
5 F. Borget, T. Chiavassa and J.-P. Aycard, *Chem. Phys. Lett.*, 2001, **348**, 425–432.
6 A. Pelmenschikov and H. Ogasawara, *J. Phys. Chem. A*, 2002, **106**, 1695–1700.
7 C. Manca, P. Roubin and C. Martin, *Chem. Phys. Lett.*, 2000, **330**, 21–26.
8 P. K. Hudson, M. A. Zondlo and M. A. Tolbert, *J. Chem. Phys. A*, 2002, **106**, 2882–2888.
9 K. Jaeger, M. Wierzejewska-Hnat and O. Schrems, *Proceedings of 8th International Conference on Fourier Transform Spectroscopy, 1–6 Sept 1991*, SPIE, vol. 1575, pp. 331–332.
10 L. Schriver, C. Barreau and A. Schriver, *Chem. Phys.*, 1990, **140**, 429–438.
11 A. J. Sedlacek and C. A. Wight, *J. Phys. Chem.*, 1989, **93**, 509–511.
12 M. W. Schmidt, K. K. Baldridge, J. A. Boatz, S. T. Elbert, M. S. Gordon, J. H. Jensen, S. Koseki, N. Matsunaga, K. A. Nguyen, S. J. Su, T. L. Windus, M. Dupuis and J. A. Montgomery, *J. Comput. Chem.*, 1993, **14**, 1347–1363.
13 PC GAMESS home page: http://classic.chem.msu.su/gran/gamess/index.html.
14 M. J. Frisch, G. W. Trucks, H. B. Schlegel, P. M. W. Gill, B. G. Johnson, M. A. Robb, J. R. Cheeseman, T. Keith, G. A. Petersson, J. A. Montgomery, K. Raghavachari, M. A. Al-Laham, V. G. Zakrzewski, J. V. Ortiz, J. B. Foresman, J. Cioslowski, B. B. Stefanov, A. Nanayakkara, M. Challacombe, C. Y. Peng, P. Y. Ayala, W. Chen, M. W. Wong, J. L. Andres, E. S. Replogle, R. Gomperts, R. L. Martin, D. J. Fox, J. S. Binkley, D. J. Defrees, J. Baker, J. P. Stewart, M. Head-Gordon, C. Gonzalez, and J. A. Pople, *Gaussian 94, Revision D.1*, Gaussian, Inc., Pittsburgh PA, 1995.
15 S. B. Boys and F. Bernardi, *Mol. Phys.*, 1970, **19**, 553–567.
16 L. Gonzalez, O. Mo and M. Yanez, *J. Comput. Chem.*, 1997, **18**, 1124–1135.
17 J. A. Dobado and J. Molina, *J. Phys. Chem.*, 1994, **98**, 1819–1825.
18 A. Engdahl and B. Nelander, *Phys. Chem. Chem. Phys.*, 2000, **2**, 3967–3970.
19 A. Engdahl, B. Nelander and G. Karlstroem, *J. Phys. Chem. A*, 2001, **105**, 8393–8398.
20 M. E. Jacox, *Vibrational and Electronic Energy Levels of Polyatomic Transient Molecules in NIST Chemistry WebBook, NIST Standard Reference Database Number 69*, ed. P. J. Linstrom and W. G. Mallard, 2001, National Institute of Standards and Technology, Gaithersburg MD, 20899 (http://webbook.nist.gov).
21 K. P. Huber and G. Herzberg, *Constants of Diatomic Molecules in NIST Chemistry WebBook, NIST Standard Reference Database Number 69*, ed. P. J. Linstrom and W. G. Mallard, 2001, National Institute of Standards and Technology, Gaithersburg MD, 20899 (http://webbook.nist.gov).
22 J. E. Del Bene and M. J. T. Jordan, *J. Mol. Struct.: THEOCHEM*, 2001, **573**, 11–23.
23 J. Lundell, S. Jolkkonen, L. Khryachtchev, M. Petersson and M. Räsänen, *Chem. Eur. J.*, 2001, **7**(8), 1670–1678.

24 J. R. Goebel, B. S. Ault and J. E. Del Bene, *J. Phys. Chem. A*, 2001, **105**, 6430–6435.
25 B. Nelander, *J. Phys. Chem. A*, 1997, **101**, 9092–9096.
26 J. A. Pople, K. Raghavachari, M. J. Frisch, J. S. Binkley and P. v. R. Schleyer, *J. Am. Chem. Soc.*, 1983, **105**, 6389–6399.
27 B. S. Jursic, *J. Mol. Struct.: THEOCHEM*, 1997, **417**, 81–88.
28 T. Okajima, *J. Mol. Struct.: THEOCHEM*, 2001, **572**, 45–52.
29 S. Pehkonen, M. Petterson, J. Lundell, L. Khriachtchev and M. Räsänen, *J. Phys. Chem. A*, 1998, **102**, 7643–7648.